Chapter 7
Application of Analytical Hierarchy Process (AHP) and Frequency Ratio (FR) Model in Assessing Landslide Susceptibility and Risk

Abstract To prepare landslide susceptibility map of the Shivkhola watershed, one of the landslide prone part of Darjiling Himalaya, RS and GIS tools were being used to integrate 10 landslide triggering parameters like lithology, slope angle, slope aspect, slope curvature, drainage density, lineament, upslope contributing area (UCA), road contributing area (RCA) settlement density, and land use and land cover (LULC). *Analytical Hierarchy Process* (AHP) was applied to quantify all the factors by estimating factors weight on MATLAB Software with reasonable consistency ratio (CR). *Frequency ratio model* (FR) was used to derive class frequency ratio or class weight incorporating both pixels with and without landslides and to determine the relative importance of individual classes. All the required data layers were prepared in consultation with SOI Topo-sheet (78B/5), LIIS-III Satellite Image (2010) by using Erdas Imagine 8.5, PCI Geomatica, and ARC GIS Software. The weighted linear combination (WLC) method was followed to combine factors weight and class weight and to determine the landslide susceptibility coefficient value (LSCV or 'M') on GIS platform. Greater the value of 'M', higher is the susceptibility of landslide. The Shivkhola watershed was classified into five landslide susceptibility zones by averaging window lengths of 3, 5, 7, and 9 and taking into account the landslide threshold boundaries value of 7.05, 9.29, 11.5, and 13.8. The overall classification accuracy rate is 92.22 % and overall Kappa statistics is 0.894. The elements like weighted LULC map, RCA (road contributing area) map and settlement density map were developed and their weighted linear combination was performed to prepare *landslide risk exposure* map. Then by integrating *landslide susceptibility map* and *landslide risk exposure map* landslide hazard risk co-efficient values were derived and a classification was incorporated on ARC GIS Platform to prepare *landslide hazard risk map* of the Shivkhola watershed. To evaluate the validity of the *landslide hazard risk map*, probability/chance of landslide hazard risk event has been estimated by means of frequency ratio (FR) between landslide hazard risk area (%) and number of risk events (%) for each landslide hazard risk class. Finally, an accuracy assessment was made through a comparative study between true GPS derived data and a set of randomly selected pixels points from the classified image corresponding to the true data from 50 locations on ERDAS Imagine (8.5) which depicts that the classification accuracy of the *landslide hazard risk map* was 92.89 with overall Kappa statistics of 0.8929.

S. Mandal and R. Maiti, *Semi-quantitative Approaches for Landslide Assessment and Prediction*, Springer Natural Hazards, DOI 10.1007/978-981-287-146-6_7

Keywords Landslide susceptibility · Landslide risk · Analytical hierarchy process (AHP) · Frequency ratio (FR) · RS and GIS · Accuracy assessment

7.1 Introduction

The identification of the causative factors is the basis of many methods of landslide susceptibility assessment. In most of the cases, the landslide is the critical mechanism of erosional processes and in such condition, landslide is inevitable and necessary part of the natural landscape process system. Although the occurrences of landslide hazards and its impact on human society cannot be prevented fully by analyzing the slope stability condition, but the better understanding of geo-technical attributes of the soil can contribute to greater knowledge and understanding about the spatial distribution of slope instability which are very much essential for land use planning. Landslides are the results of two interacting sets of forces; *the precondition factors*, naturally induced which govern the stability conditions of slopes, and *the preparatory and triggering factors,* induced either by natural factors or by human intervention. Landslide analysis is mainly done by assessing Susceptibility, Hazard and Risk (Einstein 1988). RS and GIS based landslide hazard zonation approach had been studied by Anabalangan (1992), Muthu and Petrou (2007) and Caiyan and Jianping (2009). Rowbothan and Dudycha (1998), Donati and Turrini (2002), Lee and Choi (2003), Lee et al. (2004a, b), Lee and Pradhan (2006, 2007), Pradhan and Lee (2010a, b, c), Sarkar and Kanungo (2004), Sharifikia (2007), Pande et al. (2008) and Nithya and Prasanna (2010) studied and applied the probabilistic model for landslide susceptibility and risk evaluation. Guzzetti et al. (1999a) summarized many landslide hazard evaluation studies. Jibson et al. (2000) and Zhou et al. (2002) applied the probabilistic models for landslide risk and hazard analysis. Atkinson and Massari (1998) and Vijith and Madhu (2008) introduced the logistic regression model for landslide hazard mapping. Landslide hazards were evaluated by using fuzzy logic, and artificial neural network models were used in the works of Gokceoglu et al. (2000) and Pistocchi et al. (2002). Landslide Susceptibility mapping using either multivariate or bivariate statistical approach considered the historical link between landslide controlling factors and the distribution of landslides (Guzzetti et al. 1999b, c).

The models in connection to the slope stability, shallow and deep seated landslides were introduced and verified by Varnes (1958), Young (1963), Vanmarcke (1977), Burton and Bathrust (1998), Bradinoni and Church (2004). The geotectonic factors of slope instability were studied in details by Brudsen (1979), Windisch (1991), Carson (1975, 1977) and Borga et al. (1998). Comprehensive list of stability factors commonly employed in the factors mapping approach was prepared by Crozier (1986) and Tiwari and Marui (2001, 2002, 2003, 2004). *Analytical Hierarchy Process* (AHP), a semi-quantitative method based on decomposition, comparative judgement, and synthesis of priorities are often very much useful for

regional susceptibility studies as suggested by Saaty (1980), Soeters and Van Westen (1996), Mwasi (2001), Nie et al. (2001), Yagi (2003), Komac (2006), Yalcin and Bulut (2007), Kamp et al. (2008) and Yalcin (2008). The frequency ratio (FR) model has become very popular as realistic quantitative approach in the landslide susceptibility mapping. This approach is related with the historical landslide events and their areal coverage. Lee and Pradhan (2007) argued that frequency ratio model provides a correlation between the historical slide locations and various influencing factors under consideration. Intarawichian and Dasananda (2011) applied frequency ratio model to analyze slope instability and ascribed the model as a popular quantitative method.

The present study deals with the estimation of factor's weight and class frequency ratios using 'AHP' and 'FR' model respectively. Integration between factor's weight (FW) and class frequency ratio (FR) was performed with the help of a *liner combination model.* This is done to derive pixel wise landslide susceptibility index values (LSIV) on GIS platform and to prepare landslide susceptibility map.

Landslide hazard risk analysis is the assessment of the probability of the damage of land and associated resources of different magnitudes that may occur in a region due to landslides. Earlier attempts to reduce landslide risk is largely a history of management of landslide terrain by construction of protective structures or monitoring and warning systems, or the ever-increasing sophisticated methods for mapping and delineating areas prone to landslide (Dai and Lee 2002). Risk of landslide is normally defined as the expected number of lives lost, persons injured, property damages and disrupted economic activities due to particular landslide hazard for a given area and reference period (Varnes 1984). To reduce the risk from the landslide events, the knowledge about potentiality to slope instability is crucially needed. Information of landslide events are described in the form of landslide susceptibility map of the concerned region and the preparation of this map depends largely on the complex sets of knowledge of controlling slope movement factors. Landslide analysis is mainly done by assessing susceptibility, hazard and risk (Einstein 1988). The process of creating the maps involves several qualitative or quantitative approaches (Soeters and Van Westen 1996; Guzzetti et al. 1999a; Van Westen et al. 2008). Jibson et al. (2000), Praise and Jibson (2000) and Zhou et al. (2002) have applied the probabilistic models for landslide risk and hazard analysis. *Landslide hazard risk map* was made integrating *landslide susceptibility map* and *landslide risk exposure map* on ARC GIS platform to identify the spatial distribution of potential risk prone area in a representative drainage basin, over which the attributes of land, soil and water exhibit a spatial order away from the water divide in an interacting combination with human actions.

Tectono-statigraphically, the study area, Shivkhola Watershed is located in the southern escarpment slope of Darjiling Himalaya, where high grade metamorphic rocks of the Darjiling and Chungthang groups are thrusted over low grade metamorphic rocks of the Daling Group along the *MCT* (Main Central Thrust, Mallet 1875; Sinha-Roy 1982). Main Central Thrust (*MCT*) and Main Boundary Thrust (*MBT*) are passing through the study area (Fig. 7.1). The *MCT* (a major ductile shear zone) has divided two major litho-tectonic units, the Higher Himalayan

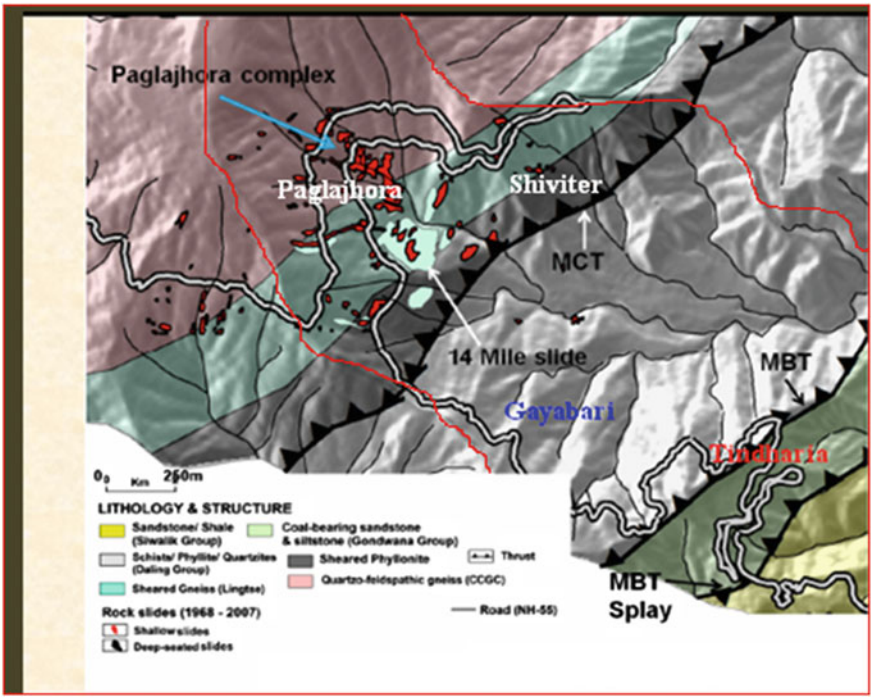

Fig. 7.1 Tectono-stratigraphy and past landslide in the Shivkhola watershed (Mandal and Maiti 2013)

Crystalline Sequence (*HHCS*) and the Lesser Himalayan Sequence (*LHS*) *in Darjiling Himalaya*. The *HHCS* comprises of quartzo-feldspathic gneisses of both igneous and sedimentary origin which suffers high grade of metamorphism (Catlos et al. 2001). The *LHS* is dominated by garnet-biotite-mica schist and chlorite schists in the upper part and slates and phyllites in the lower. The picturesque landslide affected areas are Paglajhora, Tindharia, Mahanadi, Jogmaya and Shiviter. During rainy season water percolates through the exposed rock joints and entrains the finer particles and reduces the cohesive strength of the soil.

The rapid urbanization and expansion of tourism in Darjiling Himalaya are putting unprecedented pressure on land and soil with the gradual elimination of vergin forest land after independence. Lack of land use planning coupled with vulnerable geological structure and heavy frequent rainfall have led to the formation of vicious cycle of soil erosion and landslide during and after monsoon seasons, causing devastating damage to human lives and properties. Significant studies in Darjiling Himalaya identified the causes and consequences of major landslide

occurrences phenomena (Dutta 1966). Since 1968, the Shivkhola watershed of Darjiling Himalaya faced 128 approachable landslide events, of which 76 events were identified as reactivated (not 70 m away from old slided area) and 52 as fresh events (70 m away from the old slided area) (Appendix D, Table D.1). The considered landslide events took place in 16 years and out of which 12 years were recognized as the major landslide years. All the landslide events occurred during the monsoon period being triggered by continuous and heavy showers. Rainfall on all the major landslide events date was more than the critical rainfall calculated after Borga et al. (1998). Most of the landslide events occurred in the lithological unit of Darjeeling Gneiss, Daling, Damuda and Siwalik.

In the present study of landslide hazard risk mapping in Shivkhola Watershed of Darjiling Himalaya prioritized class ranking value (PCRV) and prioritized factors rating value (PFRV) for each thematic data layers and their consistency checking was accomplished through pair-wise comparison matrix as described by Saaty (1980, 1990, 1994), and Saaty and Vargas (2001). *Landslide hazard risk map* was made integrating *landslide susceptibility map* and *landslide risk exposure map* on ARC GIS platform to identify the spatial distribution of potential risk prone area.

In the Shivkhola Watershed, Lower Paglajhora, Tindharia, Shiviter and Mahanadi are the major and prominent landslide location sites where settlement, communication lines, and tea garden area are being affected severely. Since 1968, Paglajhora alone has had 10 landslide events, all in the above mentioned landslide event years. The majority of these landslides was dangerous as in most of the events Hill Cart Road (NH-55) was affected and the communication line between Siliguri and Darjiling was completely interrupted, from days to month. Paglajhora sinking zone faced massive slope failures in 1998, 2002, 2005 and 2011 which indicates that the occurrence of landslides in the region is ongoing. This poses a tremendous threat to upslope settlement and Hill Cart Road (life line between Siliguri and Darjiling Town). The landslide events at Tindharia also used to cut-off the Hill Cart Road and brought tremendous threat to tourists, upslope settlements and tea gardens. In Shiviter, around 8 acres of land were destroyed by the destructive slope failure in the past 10 years. The physiographic configuration (arcuate) that provide a favourable condition for producing hydrostatic pressure, proximity to Main Central Thrust (MCT) and Main Boundary thrust (MBT), intensely fractured and sheared bed rock, toe cutting and headward erosion of debris covered slope by fast flowing tributaries, immense pressure over the fragile slope materials by man-made concrete structure, moderate to steep slope gradient, improper drainage and accumulation of highly anisotropic materials with a great thickness and low shearing resistance have made these landslide locations in the Shivkhola watershed most unstable in character. The main purpose of the present study is to prepare landslide susceptibility map and landslide hazard risk map applying RS and GIS semi-quantitative approach and to compare risk dominated part of Paglajhora, Tindharia, and Shiviter with the prepared risk map by incorporating landslide inventory statistics and frequency ratio (FR) analysis.

7.2 Materials and Methods

The thematic data layers of all the landslide inducing factors were integrated to prepare landslide susceptibility map using a linear combination model in GIS. The Analytical Hierarchy Process (AHP) was used to derive prioritized factor rating value (PFRV) and a FR Model was applied to obtain prioritized class rating value (PCRV) for all the landslide triggering factors considered in the study. The integration between PFRV and PCRV were made in a linear combination model on GIS platform to estimate *landslide susceptibility index value* (LSIV) for each pixel and a suitable classification technique was incorporated to prepare the landslide susceptibility map of the Shivkhola watershed. The data used in the present study are Satellite image (IIRS P6/Sensor-LISS- III, Path-107, Row-052, date-18/03/2010), modified SRTM data with scene size 1° lat. and 1° long. (date-5th April, 2008), Google Earth Image (1st September, 2010), Geological Map (Geological Survey of India, East Kolkata) and Topographical Map (78B/5, Survey of India). Data layers for landslide inducing factors were generated using ERDAS Imagine 8.5, Arc View and ARC GIS Software.

7.2.1 Landslide Susceptibility Assessment

The following section presents the methods and results of the landslide susceptibility analyses in this study.

7.2.1.1 Determination of Landslide Triggering Factors

The landslide triggering factors were identified by interviewing the local people and an investigation of the landslide sites in the watershed through intensive fieldwork. During 10 days field work in July 2011, landslide locations were identified and marked with GPS. Lithological structure, land use and land cover type around the landslide scar, slope angle, construction of human structure and their role to promote landslide, drainage network, altitude and slope aspects were investigated to determine landslide triggering factors. The landslide triggering factors including lithology, slope angle, drainage, slope aspect, slope curvature, lineament, upslope contributing area (U.C.A.), land use/land cover, road contributing area (RCA) and settlement density were taken into account to prepare landslide susceptibility map of the Shivkhola watershed and their hierarchical arrangement was made on priority basis. Shivkhola watershed is a small mountain basin where rainfall is uniformly distributed over the entire area, so rainfall intensity was not considered in the landslide susceptibility calculation (Mandal and Maiti 2011, 2012, 2013).

7.2.1.2 Generation of Landslide Inducing Factor Maps

First, the *contour map* at 20 m interval was prepared and digitized from the SOI Topo-sheet (1987, 78B/5) at the scale of 1:50,000 and subsequently employed for generating the Digital Elevation Model (DEM) using ARC GIS Software. Then *slope gradient*, *slope curvature* and *slope aspect map* were derived from DEM and classification was made to derive all these parameters in raster value domain following the earlier works of Dhakal et al. (2000). Surface curvature is a topographic attribute that describes the convexity/concavity of a terrain surface. Curvature depicts the slope gradient or slope direction (aspect), usually in a particular direction. A positive curvature indicates that the surface is upwardly convex at a grid cell and a negative curvature indicates that the surface is upwardly concave at that grid cell. A value of zero indicates that the surface is flat. The expected values of all three output raster images for a hilly area can vary from −0.5 to 0.5; for steep, rugged mountains the value can vary between −4 and 4.

The *lithological map* of the study area was collected from Geological Survey India (GSI), Kolkata (Eastern Region) and necessary modifications were incorporated after intensive field investigation. Final lithological map was prepared and transformed into raster value domain on ARC GIS Platform. Class weight value for each lithological class was assigned according to rock mass strength, described by GSI. A Drainage density map (length of drainage/m^2) was made from the topographical map (78B/5, 1987) and classified into ten equal intervals.

The *lineament* exhibits the zone of weakness surface of some linear to curvilinear features such as fracture, joint, fault etc. in the geological structure. There are no basic differences between these three features. All these linear to curvilinear features were identified as the same deformed surface where the propensity of slope instability is very high. To generate lineament map (distance from lineament in meters) of the Shiv-khola watershed, PCI-GEOMATICA was used and in the extraction process 3 SRTM bands of wavelengths were taken into account: Near Infrared (Band-I; 0.7–1.3 μm), Red (Band-II; 0.6–0.7 μm) and Green (Band-III; 0.5–0.6 μm). The '*Lineament extraction*' algorithm was used to prepare lineament map. The study area was classified into ten classes on the basis of the distance (m) from lineaments.

Upslope Contributing Area is an effective indicator of drainage concentration over space. The place with more contributing area encompasses more soil saturation that reduces soil cohesion. The specific contributing area (total contributing area divided by the contour length) is computed by distributing flow from a pixel among its entire lower elevation neighbour pixel (Borga et al. 1998). Quinn et al. (1991) proposed that the Fraction of Flow (F_i) allocated to each lower neighbour (i) is determined by using Eq. 7.1. An upslope contributing area map was prepared based on calculated contributing area value for each (0.25 km^2) grid and it was divided into 6 equal classes (Fig. 3.7, Chap. 3).

$$F_i = \frac{\text{SiLi}}{\sum \text{SiLi}} \tag{7.1}$$

where, the summation (Σ) is for the entire lower neighbour; S is the directional slope, and L is an effective contour length that acts as the weighting factor. The value of L used here is 10 m of the pixel size of the cardinal neighbour and 14.14 m of the pixel diagonal for diagonal neighbour.

The *road contributing area* (*RCA*) *map* (Fig. 7.6) was made by multiplying road contributing length (RCL) with road contributing width (RCW) with eight equal classes from the concerned topographical sheet and it was converted into raster value domain on ARC GIS Platform. The *Settlement Density Map* (Fig. 7.4) was prepared by applying 3 × 3 karnel in ARC GIS platform and the whole basin was classified into seven equal density classes. Land use and land cover (LULC, Fig. 7.5) map of the Shivkhola watershed is prepared with the help of LISS-III Satellite Image (2010) and Google Earth Image in consultation with SOI Topo-sheet (78B/5). After verifying the ground truth with GPS a land use and land cover map is developed in GIS. The Shivkhola Watershed was classified into 10 individual land use type: (i) bare surface, (ii) agricultural land, (iii) jungle, (iv) roads, (v) settlement, (vi) tea garden, (vii) open forest, (viii) degraded forest, (ix) mixed forest and (x) dense forest (Fig. 4.2, Chap. 4).

7.2.1.3 Landslide Inventory Map

A *Landslide Distribution Map/Inventory Map* (Fig. 2.1, Chap. 2) was created to determine landslide affected area (%) and frequency of landslide for each class of the landslide inducing factors/factors. Mandal and Maiti (2011) identified major and minor landslide locations during field investigation and mapped them by evaluating the SOI topographic map (78B/5), satellite image (IRS LISS-III, 2000), SRTM data (2008), and Google Earth Image (2010). Several field investigations were conducted to identify the landslide locations and to cross-check the prepared landslide map. Then, the map was digitized and converted into raster value domain in ARC GIS Software. All the landslide triggering factor maps were linked with the prepared landslide inventory map to understand the degree of importance of each factor in landsliding.

7.2.1.4 AHP and Quantification to Each Factor Map/Prioritized Factor Rating Value

AHP is a decision making and semi-quantitative value judgement approach which serve the objectives of the decision makers. This process is employed to support the decision on the instability rank of the factors by estimating prioritized factor rating value (PFRV). In the AHP, different factor preference and their conversion into

Table 7.1 Scale of preference between two parameters

Scale	Degree of preference	Explanation
1	Equally	Two activities contribute equally to the objective
3	Moderately	Experience and judgement slightly to moderately favour one activity over another
5	Strongly	Experience and judgement strongly or essentially favour one activity over another
7	Very strongly	An activity is strongly favoured over another and its dominance is showed in practice
9	Extremely	The evidence of favouring one activity over another is of the highest degree possible of an affirmation
2, 4, 6 and 8	Intermediate values	Used to represent compromises between the references in weight 1, 3, 5, 7 and 9
Reciprocals	Opposites	Used for inverse comparison

numerical value was accomplished with the help of comparative oral judgment and synthesis of priorities. A couple comparing matrix was constructed on the basis of the preference of a factor as compared with the other factor and arithmetic mean method was applied to arrange landslide triggering factors hierarchically and to determine *prioritized factor rating value/eigenvector* (*PFRV*) with reasonable consistency ratio (CR) on MATLAB software after Saaty (1980) (Table 7.2). To develop pair-wise comparison matrix, each factor/class was rated against every other factor by assigning a relative dominant value ranging between 1 and 9 on the basis of the relative importance of the factors in terms of landslide frequency. The value also varies between the reciprocals 1/2 and 1/9 for inverse comparison (Table 7.1).

Another appealing feature of the AHP is the ability to evaluate pair-wise rating inconsistency. The eigenvalues enable to quantify a consistency measure which is an indicator of the inconsistencies or intransivities in a set of pair-wise ratings. Saaty presented that for a consistent reciprocal matrix, the largest eigenvalue λ_{Max} is equal to the number of comparisons n (Table 7.2).

In AHP, an index of consistency, known as the CR (Consistency Ratio), is used to indicate the probability that the matrix judgements were randomly generated (Saaty 1994).

$$CR = CI/RI \tag{7.2}$$

where RI is the average of the resulting consistency index depending on the order of the matrix given by Saaty and CI is the consistency index that is expressed in the following equation. If the value of CR is smaller or equal to 10 %, the inconsistency is acceptable, but if the CR is greater than 10 %, the subjective valued judgement needs to be revised.

A measure of consistency, called consistency index CI, is defined as follows:

Table 7.2 Landslide triggering factors and determined prioritized factor weights

Factors	1	2	3	4	5	6	7	8	9	10	Prioritized rating
Slope	1	2	3	4	5	6	7	8	9	9	0.2944
Lithology	1/2	1	2	3	4	5	6	7	8	9	0.2150
Drainage	1/3	1/2	1	2	3	4	5	6	7	8	0.1537
Lineament	1/4	1/3	1/2	1	2	3	4	5	6	7	0.1087
Curvature	1/5	1/4	1/3	1/2	1	2	3	4	5	6	0.0764
UCA	1/6	1/5	1/4	1/3	1/2	1	2	3	4	5	0.0535
RCA	1/7	1/6	1/5	1/4	1/3	1/2	1	2	3	4	0.0375
LULC	1/8	1/7	1/6	1/5	1/4	1/3	1/2	1	2	3	0.0266
Settlement density	1/9	1/8	1/7	1/6	1/5	1/4	1/3	1/2	1	2	0.0193
Slope aspect	1/9	1/9	1/8	1/7	1/6	1/5	1/4	1/3	1/2	1	0.0149

CI = 0.0615; R.I (random index) = 1.49 and CR = 0.0413 (consistent). *RCA* road contributing area; *UCA* upslope contributing area; *LULC* land use and land cover
Source Saaty (1980)

$$\mathrm{CI} = \lambda_{\mathrm{Max}} - \mathrm{n/n} - 1 \tag{7.3}$$

Saaty and Vargas (2001) randomly produced reciprocal matrices using scales 1/9, 1/8, 1/7, …, 1, …, 8, 9 to evaluate a so called random consistency index (RI). The average RI of 500 matrices is given in Table 7.3.

7.2.1.5 Frequency Ratio Model and Prioritized Class Rating Value

Frequency ratio (FR) model is also a well accepted and popular quantitative approach for the preparation of landslide susceptibility map. Lee and Talib (2005), Pourghasemi (2007), Lee and Pradhan (2007), Jadda (2009), Avinash and Ashamanjari (2010), Intarawichian and Dasananda (2011) successfully applied 'FR' model to generate landslide susceptibility zoning map. To obtain *frequency ratio (FR)* for each class of all the data layers a combination has been established between landslide inventory map and criterion maps using following equation.

$$\mathrm{Fr_i} = \frac{\mathrm{N_{pix(S_i)}}/\mathrm{N_{pix(N_i)}}}{\sum \mathrm{N_{pix(S_i)}}/\sum \mathrm{N_{pix(N_i)}}} \tag{7.4}$$

$\mathrm{N_{pix(S_i)}}$ The number of pixels containing slide in each class (i),
$\mathrm{N_{pix(N_i)}}$ Total number of pixels having class (i) in the whole watershed,
$\sum \mathrm{N_{pix(S_i)}}$ Total number of pixels containing landslide,
$\sum \mathrm{N_{pix(N_i)}}$ Total number of pixels in the whole area of the watershed.

Table 7.3 Random index (RI)

N	1	2	3	4	5	6	7	8	9	10	11	12	13	14	15
RI	0	0	0.58	0.90	1.12	1.24	1.32	1.41	1.45	1.49	1.51	1.53	1.56	1.57	1.59

The derived *frequency ratio* (FR) value of more than '1' indicates, strong and positive relationship between landslide occurrences in each class of the data layers and high landslide susceptibility where 'FR' value of less than '1' depicts the negative and low landslide susceptibility. In this study, 'FR' values for each class were accepted as *prioritized class rating value* (PCRV) or *prioritized class weight* (PCW).

7.2.1.6 Linear Combination Model and Landslide Susceptibility Map

Avinash and Ashamanjari (2010) and Intarawichian and Dasananda (2011) used a landslide susceptibility index value (LSIV) which is the summation of class-and factor-weighted values.

'FR' values for each class (PCRV) or prioritized class rating value, (Table G.1, Appendix G) as well as *prioritized factor's weighted values* (PFRV) for each factor map was taken into account in calculating the *landslide susceptibility index value* (*LSIV*) with the following linear combination model:

$$LSIV = \sum_{i=1}^{n} (W_i * FR_i) \times \mathrm{FV} \tag{7.5}$$

where, n: total number of factors included in the study (n = 10); $W_{i:}$ Factor's weight (PFRV), FV IS factor value, and FR_i: Class Frequency Ratio/class weight.

The 'LSIV' varied from '4.81' to '16.00'. Higher the value of 'LSIV', greater was the propensity of landslide phenomena and vice versa. The LPIV based frequency curve showed many oscillations. To classify the watershed into 5 susceptibility zones moving averages with averaging window lengths of 3, 5, 7, and 9 were considered for smoothing the frequency distribution curve (Fig. 7.2). After analyzing four new curves, the Shivkhola Watershed was classified into 5 landslide susceptibility zones i.e. very low, low, moderate, high, and very high with class boundaries were demarcated at the significant changes of gradient of the curves. The abrupt change points on frequency curve (landslide threshold boundaries) were 7.05, 9.29, 11.5, and 13.8 which were recognized as class boundaries to classify the map. A 3 × 3 'majority filter' technique was applied to the map as a post-classification filter to reduce the high frequency variation.

To verify the landslide susceptibility map, *landslide density* under each susceptibility class was computed. The landslide inventory map was crossed with prepared landslide susceptibility map to derive landslide affected pixels for each susceptibility classes (zones). Research by Sarkar and Kanungo (2004) indicates that the higher the landslide density, greater is the probability and larger the area is affected by landslide in each landslide susceptibility class.

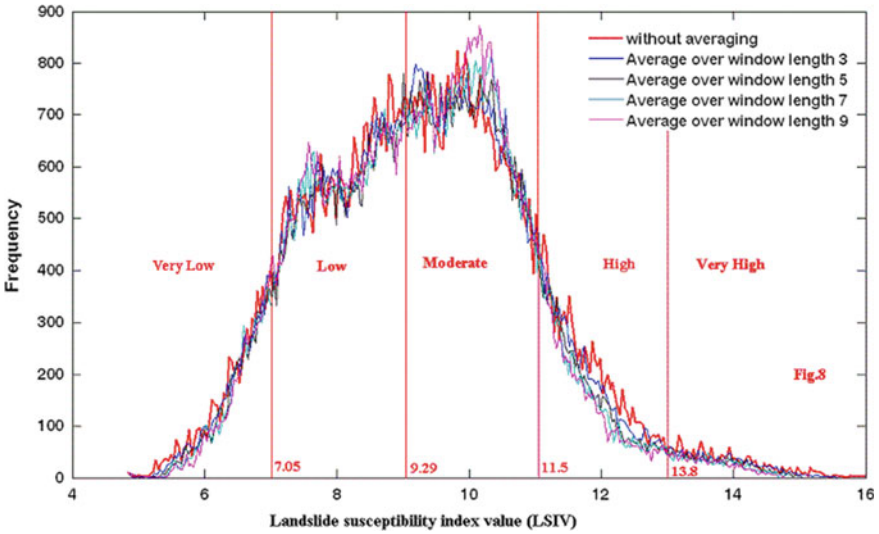

Fig. 7.2 Frequency distribution of landslide susceptibility index value of the Shiv-khola watershed in West Bengal, India

7.2.1.7 Accuracy Assessment of the Landslide Susceptibility Map with Field Data (GPS Survey)

Accuracy assessment is a general term for comparing the classification with geographical data that are assumed to be true, in order to determine the classification process that was accomplished by using Erdas Imagine (8.5). True data were derived by ground truth verification with the help of GPS from the existing 50 landslide locations. Simultaneously, a set of randomly selected 50 reference pixels points from the classified image corresponding to the true data (GPS record) were used for evaluating the validity of landslide susceptibility map after Congalton (1991).

7.2.2 Landslide Risk Assessment

In this study, landslide risk map was made with the help of following principle (Mandal and Maiti 2012).

Landslide Hazard Risk = Landslide susceptibility × Landslide Risk Exposure/ Intensity of Risk Elements.

The entire methodology to prepare the *landslide hazard risk map* of the Shiv-khola Watershed could be summarized under following heads (Fig. 7.3).

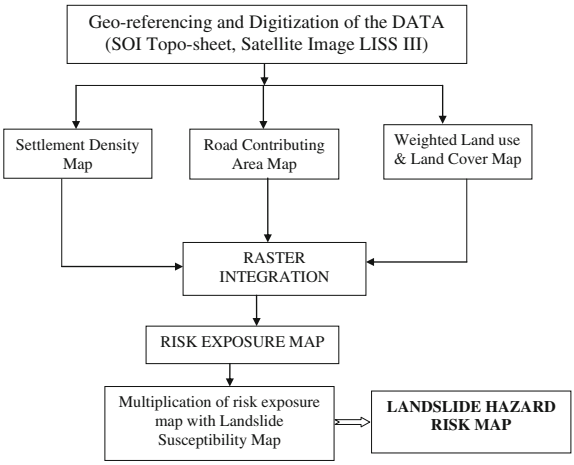

Fig. 7.3 Methodology of landslide hazard risk map

7.2.2.1 Preparation of Weighted Risk Factor/Element Maps (Weighted Land Use/Land Cover Map, Road Contributing Area Map and Settlement Density Map)

In the present study, land use and land cover, road network, and settlement were considered as important risk factors/elements because these three are worst affected by landslide events in the study area. To derive the weighted risk factor maps the developed numerical scale of 1–10 was applied to assign the scores for each class of the risk factor maps. *Weighted land use/land cover map* (Fig. 7.5) is the expression of the intensity of risk induced land use pattern in the Shivkhola watershed. A weighted land use/land cover map was developed assigning more weightage values considering the landslide contributing units to the significant landslide triggering land use pattern i.e. tea garden area, degraded forest, bare surface and agriculture. Weighted value to each class/range of the road contributing area (RCA) map was assigned considering the intensity and impact of road network on landslide and thus a *weighted road contributing area map* (Fig. 7.6) was made on GIS platform. *Settlement Density Map* was prepared by assigning more weighted values to high density class and low for low density class for raster integration and a *weighted settlement density map* (Fig. 7.4) was made accordingly. Three risk factor maps were classified into low, moderate and high intensity zones.

7.2.2.2 Integration Between Weighted Land Use and Land Cover, Road Contributing Area and Settlement Density and the Development of Risk Exposure Map

To integrate risk factor maps prioritized class rating values (PCRV) and prioritized factor rating value (PFRV) were obtained for each class and each risk factors maps developing *couple-comparing matrix* (Table 7.4) according to Saaty (1980). Then,

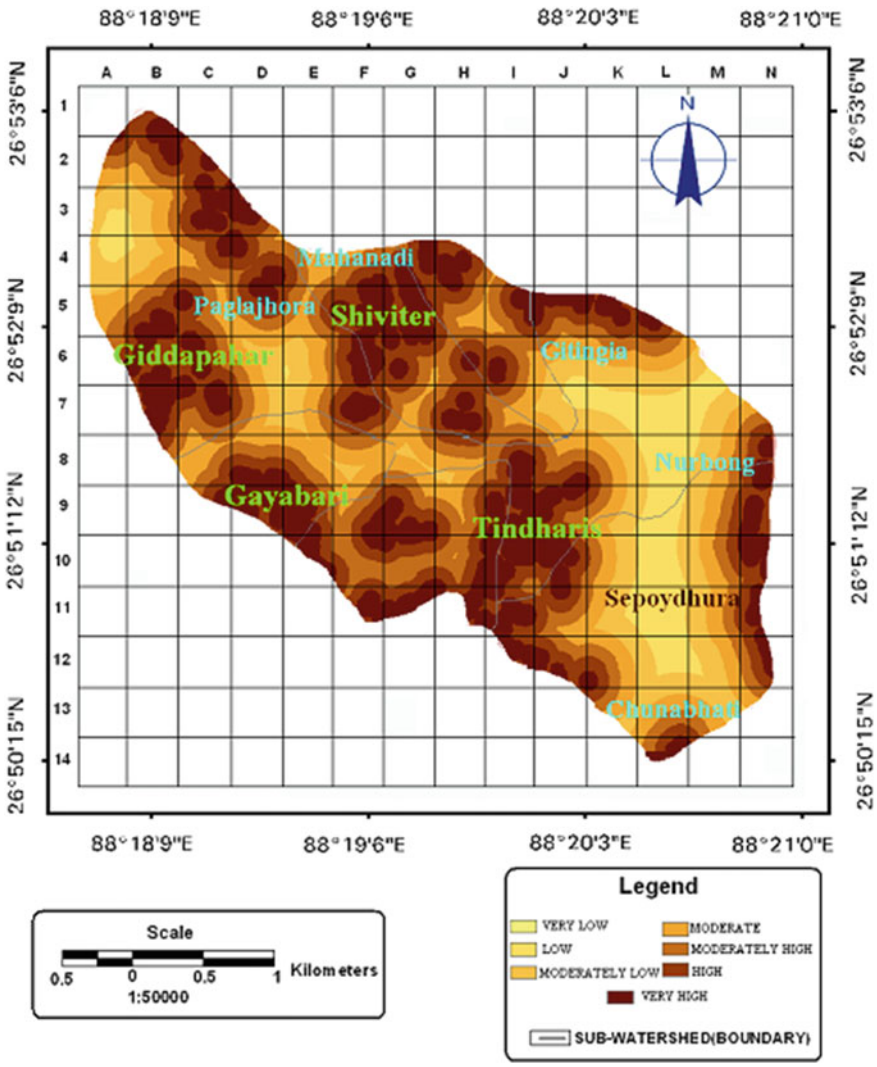

Fig. 7.4 Settlement density map

a linear combination model was performed on ARC GIS platform to derive *landslide risk exposure co-efficient value*. The derived *landslide risk exposure co-efficient value* ranges between 0.19 and 7.24 and here the values of 0.75, 1.45, 2.55, 3.85, 4.90, and 6.15 were taken into account as threshold points to classify the watershed into 7 landslide risk intensity zones. Risk exposure map (Fig. 7.7) shows the intensity of risk elements over the space which were delineated here as very low to very high ranges. The intensity of risk elements are high to very high at Tindharia Upper as well as Lower, very few parts at Gayabari upper slope, Giddapahar, Shiviter, and upper Paglajhora.

Table 7.4 Determined prioritized class rating value (PCRV) and prioritized factor rating value (PFRV) of three landslide hazard risk element maps

Weighted LULC map	Low		Moderate		High	Very high		PFRV-0.691
PCRV	0.06		0.12		0.25	0.55		
Weighted RCA map	Very low	Low	ML	M	MH	H	VH	PFRV-0.218
PCRV	0.02	0.04	0.05	0.09	0.13	0.24	0.43	
Weighted settlement density map	Very low	Low	ML	M	MH	H	VH	PFRV-0.091
PCRV	0.03	0.04	0.05	0.11	0.14	0.27	0.37	

PCRV prioritized class rating value, *PFRV* prioritized factor rating value, *LULC* land use and land cover, *RCA* road contributing area, *ML* moderately low, *M* moderate, *MH* moderately high, *H* high, *VH* very high

7.2.2.3 Preparation of Landslide Hazard Risk Map

The prioritized class rating value (PCRV) against each class of landslide susceptibility map and risk exposure map were estimated by developing couple-comparing matrices on MATLAB Software (Table 7.5) after Saaty (1980). Then, raster integration between *landslide susceptibility* and *landslide risk exposure* was performed by overlay analysis on ARC GIS platform and finally *landslide hazard risk co-efficient* (R) values were derived for each pixel. To classify 'R' value the same method was followed like the landslide susceptibility map and the Shivkhola Watershed was divided into four landslide hazard risk zones i.e. low, moderate, high and very high.

7.2.2.4 FR Study to Establish the Validity of Landslide Hazard Risk Zones

To evaluate the validity of landslide hazard risk map *frequency ratio* (FR) value was estimated for each landslide hazard risk class by means of a ratio between landslide hazard risk area (%) and landslide hazard risk events (%). The 'FR' value approaching towards '0' indicates lower landslide probability and the value approaching away from '0' or toward '1' or more than '1' denotes greater chances of landslide risk event in future. The records of the landslide hazard risk events in the unstable terrain of the Skivkhola watershed were collected from the study accomplished by Basu and Ghatowar (1988), Basu and Sarkar (1985, 1988), Basu and Ghosh (1993), Basu and Maiti (2001), Maiti (2007a, b), Ghosh et al. (2009), and author himself that were taken into account to estimate frequency ration (FR). The records depict that since 1968–2011, the Shivkhola watershed faced 128

Table 7.5 Prioritized class rating value (PCRV) of landslide susceptibility and landslide risk exposure with consistency ratio (CR)

Landslide susceptibility map	Very low (VL)	Low (L)	Moderately low (ML)	Moderate (M)	MH	H	VH	Consistency ratio (CR) = 0.02
PCRV	0.02	0.04	0.12	0.13	0.17	0.19	0.33	
Landslide risk exposure map	Very low (VL)	Low (L)	Moderately low (ML)	Moderate (M)	MH	H	VH	Consistency ratio (CR) = 0.049
PCRV	0.027	0.036	0.053	0.103	0.143	0.266	0.376	

approachable landslide events and amongst them 76 events were treated as reactivated (not 70 m away from old slided area) and 52 as fresh events (70 m away from the old slided area) (Appendix D, Table D.1). Out of 16 prominent landslide events year during the period 1968–2011, 12 years had been recognized as the major landslide hazard risk events years because in these years destructive landslide events completely cut-off communication lines, destroyed human settlements, reduced tea garden area and threatened human lives and properties severely. Considering 36 landslide hazard risk events which occurred within 12 landslide risk event years at different parts of the Shivkhola 'FR' values were derived and probable chances of future hazard risk events were estimated for each landslide hazard risk zone.

7.2.2.5 Accuracy Assessment of the Landslide Hazard Risk Map with Field Data (GPS Survey)

The accuracy assessment of the landslide hazard risk map was made by using Erdas Imagine (8.5). Accuracy assessment is a general term for comparing the classification with geographical data that are assumed to be true, in order to determine the classification process. Basically, the true data were derived for ground truth verification with the help of GPS from the existing/active 50 landslide location with risk elements (settlement, road and tea and agriculture). Simultaneously, a set of randomly selected 50 reference pixels points from the classified image corresponding to the true data (GPS record) were used for evaluating the validity of landslide hazard risk map (Congalton 1991).

7.3 Result and Discussion

7.3.1 Relationship Between Landslide Susceptibility and Landslide Triggering Factors

Landslide susceptibility map of the Shivkhola Watershed was the product of an interaction between factors and existing landslide. *Slope gradient* (Fig. 2.6, Chap. 2) of the watershed varies from very gentle gradient (around 10°) in the mid central and mid-lower part to that of high (more than 60°), towards the marginal part/water divide. Most of the landslide phenomena were found in the area of above 35° slope gradient where class weight value ranges between 5.35 and 77.56 (Appendix G, Table G.1). South, south east, north, east and north easterly facing slope (Fig. 2.7, Chap. 2) were registered with highest class weight values of 29.23, 23.63, 69.63, 53. 51, and 14.86 respectively. All these slope facets were associated with moderate to high landslide susceptibility and large number landslide events. The derived 'FR' and class weight values revealed that high to very high landslide susceptibility zones are characterized by high *positive* and *negative curvature.* Lower Paglajhora, Gayabari

(Lower), Shiviter (Lower), Tindharia T.E. were characterized by upwardly concave or negative curvature and highest class weight value ranging from 52.09 to 165.71. The marginal part of the watershed mainly Upper Paglajhora, 14 miles (upslope) bustee, Gayabari (Upper), and Tindharia (Upper) registered high positive curvature (Fig. 2.8, Chap. 2) with maximum landslide frequency and class weight of more than 40. Lithologically, Darjiling Gneiss, Gorubathan, Lingste Granite and Reyang Formation (Fig. 2.4, Chap. 2) showed the maximum number of landslide phenomena. Probability of Landslide phenomena was very high for the lithological composition of gneiss, mica-schist and granulite. Class weight values of Lingtse Granite, Gorubathan Formation and Chungtung Formation were 48.98, 50.31 and 23.10 respectively (Table G.1, Appendix G). All these lothological groups were accompanied with large number of landslide activities and greater chances of landslip probability in future. *Drainage density* (Fig. 3.6, Chap. 3) was very high at Lower Paglajhora, Gayabari and Shiviter T.E. which were attributed by high landslide susceptibility and high frequency ratio (>2.5). The value of *the drainage density* increased away from the marginal part to the central part. The area having more that 11 km length of drainage/km^2 were attribute with highest class weight (>140) and greater probability of landslide phenomena. The values of *Upslope Contributing Area* (UCA) increases away from the water divide and the maximum of 20.98 km^2 experienced the lower most portion of the watershed (Fig. 3.7, Chap. 3). The upslope contributing area having less than 5 km^2 experienced less saturation excess run-off and less intensity of landslide. The more contributing areas were registered along the main rivers that had maximum length and thus maximum flow. The study envisaged that the place with the UCA of 5.00–10.00 km^2 and 10.00–15.00 km^2 were attributed as high 'FR' value of 1.21 and 1.48 and class weight values of 20.93 and 48.39 respectively. These places were very much prone to landslide. In Shivkhola Watershed tea garden, jungle, roads and settlement (Fig. 7.5) were characterized by high 'FR' of 1.23, 1.15, 1.98 and 1.14 and highest class weight of 23.73, 15.62, 99.31 and 14.09 (Table G.1, Appendix F). The analysis showed that tea garden, road and settlement were dominated by high intensity of landslide and could be treated as maximum probable areas of landslide occurrences. Road contributing area (RCA) was high at the places of Tindharia, Paglajahora, Mahanadi and Shiviter where the landslide frequency was also very high (Fig. 7.6). At all those places the RCA ranged from 0.008 to 0.014 km^2 and the class weight value ranged between 29.84 and 169. 12. In the study area, construction of roads and slope modification caused by human intervention were responsible for slope instability. The moderate to high intensity of human settlement at Tindharia, Gayabari, Shiviter, Mahanadi and Lower Paglajhora (Fig. 7.4) depicted high 'FR' and maximum class weight as well as greater probability of landslip (Fig. 7.7).

In Shivkhola Watershed, Lower Paglajhora, Shiviter and Tindharia were very highly susceptible to landslide; Upper Paglajhora, Gayabari, 14 Miles Bustee and Nurbong T.E. were characterized by high landslide susceptibility; Mahanadi and Giddapahar were of moderate landslide potentiality; and marginal waxing slope of water divide and low-central wanning slope were registered with low landslide susceptibility (Fig. 7.8).

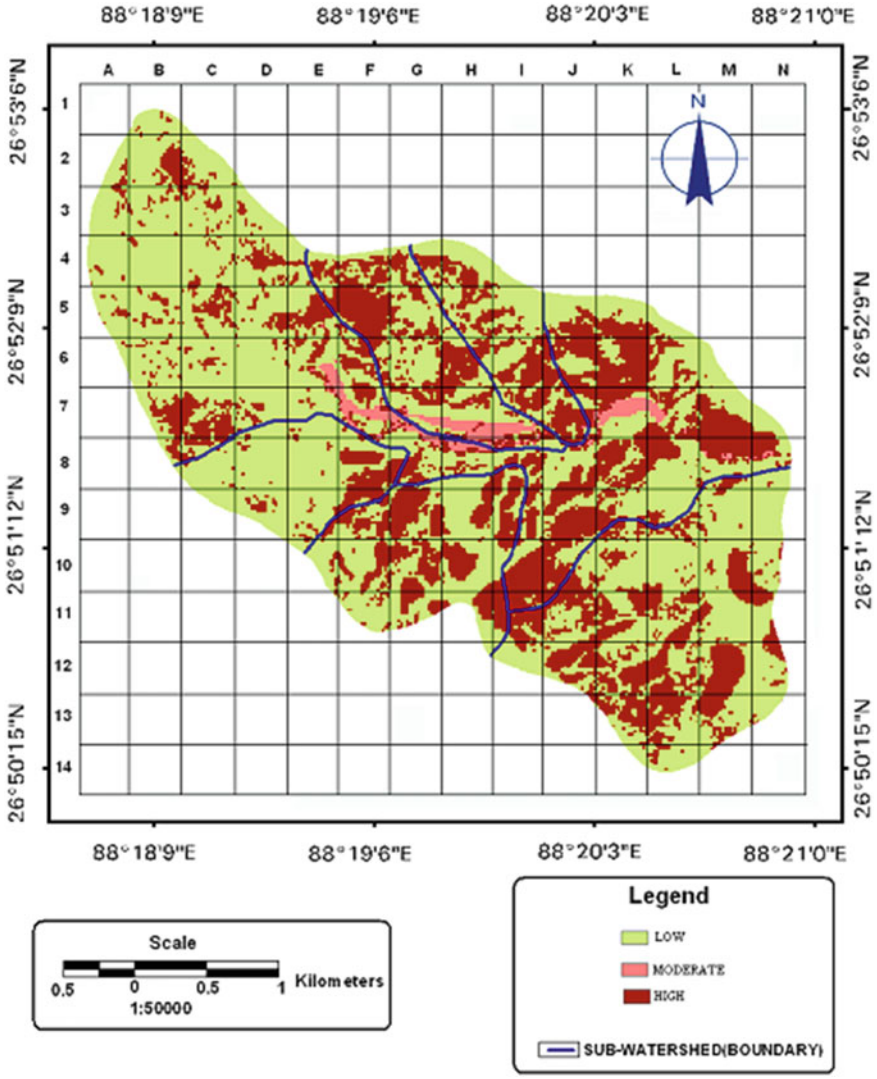

Fig. 7.5 Weighted land use and land cover map

The study revealed that around 50 % area of the Shivkhola watershed was classified as being in the moderate to very high landslide susceptibility with 71 % landslide phenomena. Low to very low susceptibility zones together accommodate 27 % of the landslide phenomena (Table 7.6). Landslide density in each susceptibility class was derived to evaluate the intensity of landslide activities. The landslide density value ranges from 0.031 to 0.25. The calculated density value of

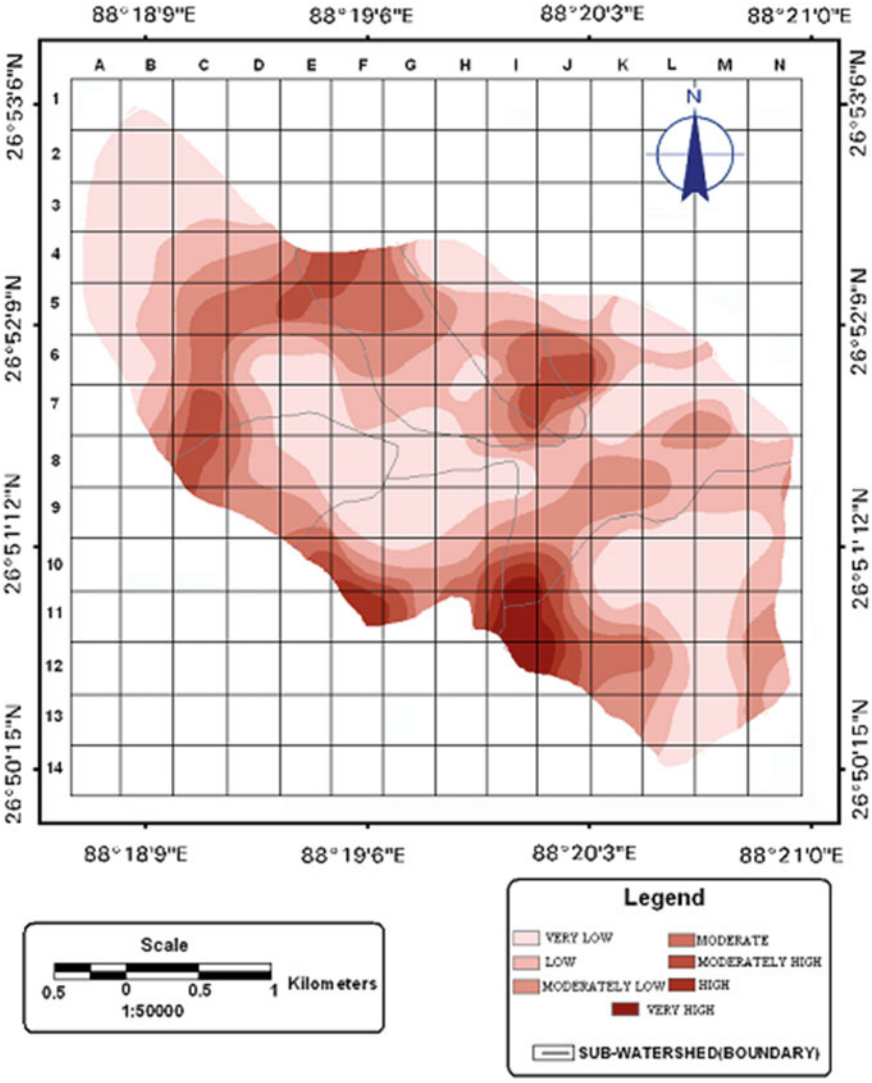

Fig. 7.6 Weighted road contributing area map

0.25 and 0.15 for very high and high landslide susceptibility zones of the watershed depicts the higher intensity of landslide activities compared to other landslide susceptibility zones. Here, frequency study shows that more than 19.58 % area is attributed with high to very high landslide probability, around 48.8 % with moderate landslide probability and remaining area with low landslide probability (Table 7.6). In landslide susceptibility classes of high and very high, the 'FR' values are 2.41 and 3.39 that indicate greater chances of landslide probability. The determined landslide density and frequency ratio reveals that the areas with high

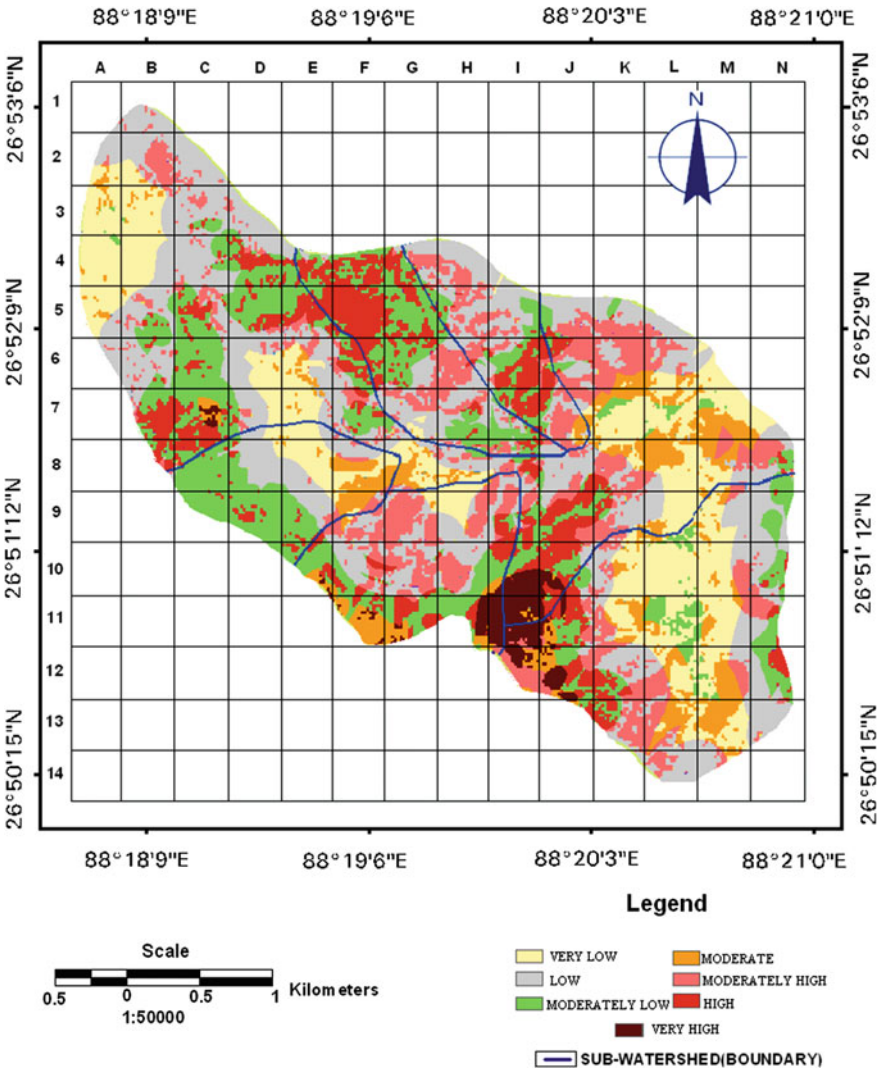

Fig. 7.7 Risk exposure/intensity map

and very landslides susceptibility are expected to have fresh landslide phenomena and here lies the validity of the present landslide susceptibility mapping approach.

A relationship was established between landslide potential index and landslide affected pixels which show that 27.22, 45, 50.03, 76.03 and 95.62 % landslide affected areas are distributed in 8.75, 28.66, 45, 78 and 92 % landslide susceptible areas. Around 35 % landslide affected pixels are distributed in 27 % of high to very high landslide potentiality zones that indicate the higher probability of landslide activities (Fig. 7.9). On the other hand 73 % landslide susceptible areas are attributed with 65 % landslide affected pixels.

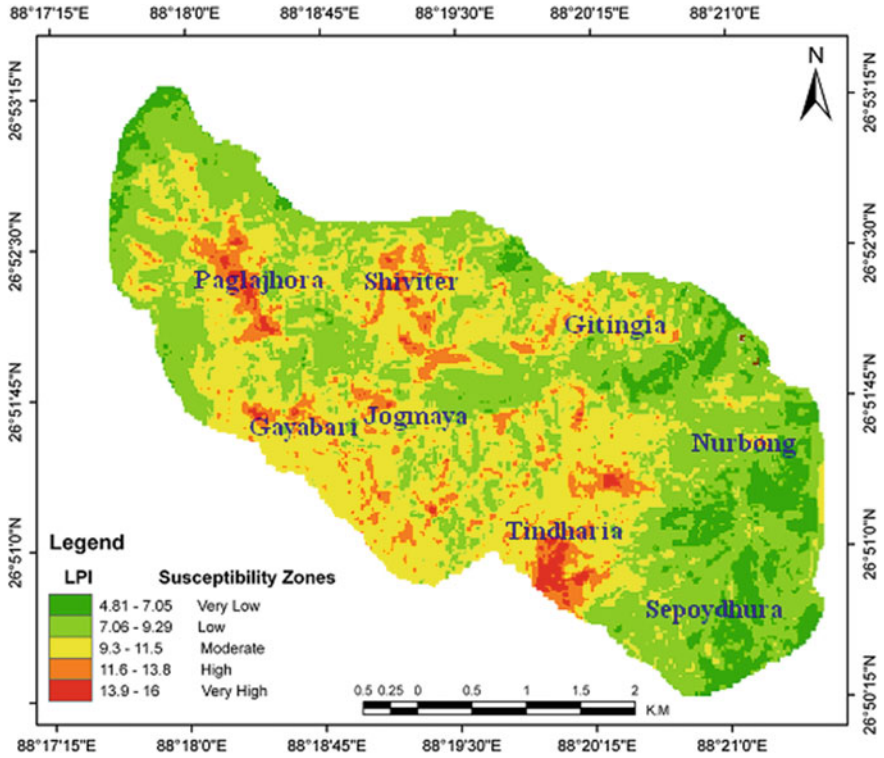

Fig. 7.8 Landslide susceptibility map

Table 7.6 Relationship between landslide susceptibility (%), landslide frequency (%) and frequency ratio (FR) and landslide density

Landslide susceptibility	Pixel (15 × 15 m) (b)	% (B)	Landslide pixel (15 × 15 m)(a)	% (A)	Frequency ratio (FR) (A/B)	Landslide density (a/b)
Very low	7,707	9.03	245	4.47	0.50	0.031789282
Low	35,386	41.46	1,247	22.74	0.54	0.035239925
Moderate	34,364	40.26	2,676	48.8	1.21	0.077872192
High	6,932	8.12	1,074	19.58	2.41	0.154933641
Very high	964	1.30	242	4.41	3.39	0.251037344

7.3.2 Accuracy Result of Landslide Susceptibility Map

The comparison between true data and randomly selected data from the classified image was made on GIS Platform that showed the overall classification accuracy of 92.22 % and overall Kappa Statistics was 0.894. The class wise accuracy result is shown in Table 7.7 that indicates acceptable results.

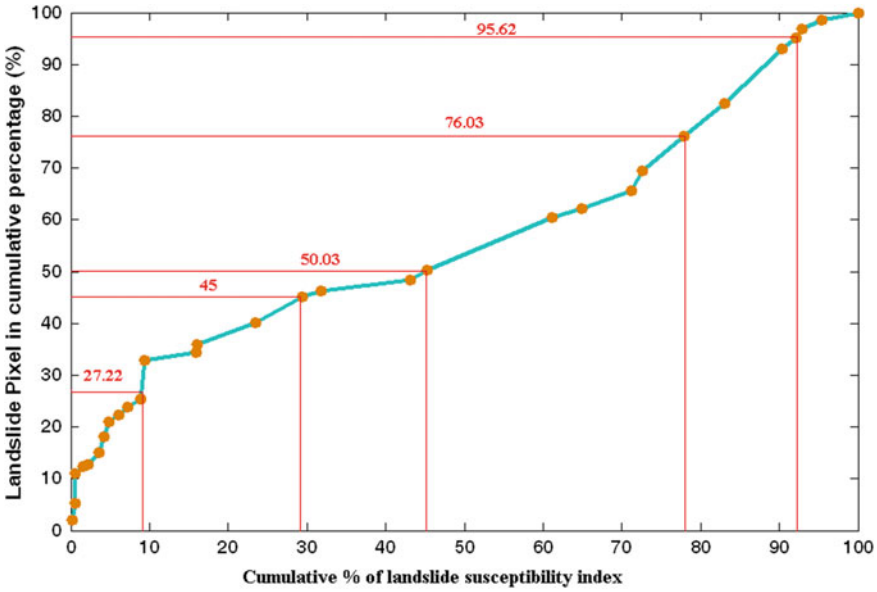

Fig. 7.9 Pixel wise distribution of landslide potentiality index

Table 7.7 Accuracy assessment/comparison of landslide susceptibility with field data

Class name	Classified total	Number correct	Producers correct	Users accuracy	Accuracy total
Very low	0	5	0	0.00	0.00
Low	4	3	0	75.00	0.00
Moderate	11	10	9	90.91	90.00
High	16	15	13	93.75	86.67
Very high	19	17	17	89.47	100.00
Total	50	50	39		
Overall classification accuracy = 92.22 %					
Overall Kappa statistics = 0.894					

7.3.3 Analysis of Landslide Hazard Risk

Study represents that the watershed is dominated by high landslide hazard risk followed by very high, moderate and low landslide hazard risk. In terms of areal coverage, 17.92, 25.37, 29.35 and 27.34 % area of the watershed is recognized by low, moderate, high and very high landslide hazard risk respectively (Fig. 7.10). Figure 7.11 shows the spatial distribution of landslide hazard risk where Lower Paglajhora, Tindharia and Shiviter are registered with high risk exposure due to

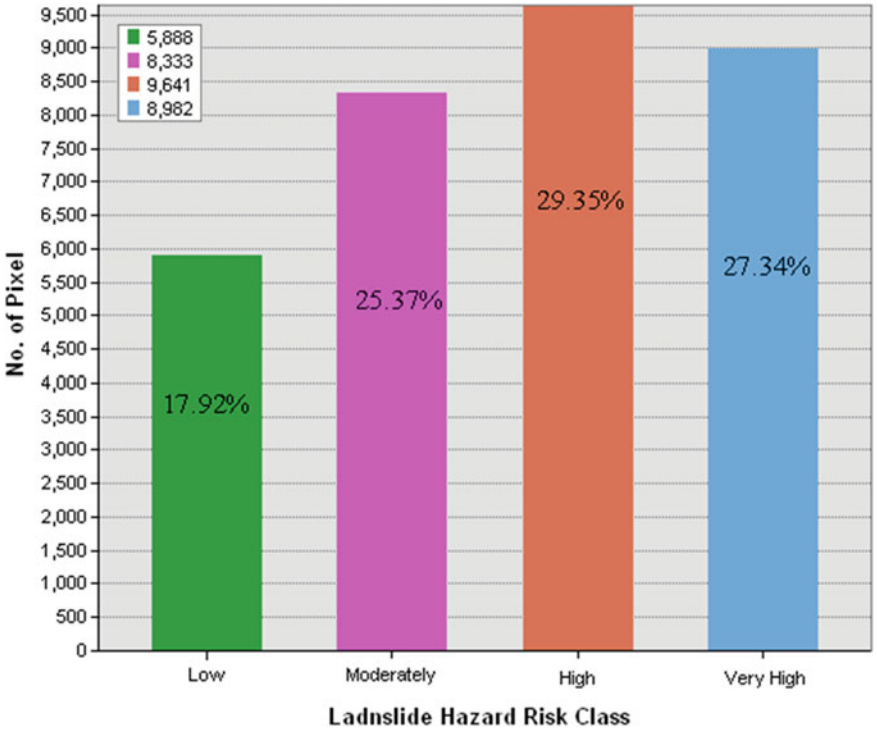

Fig. 7.10 Distribution of pixel/area (%) within landslide hazard risk classes

high intensity of risk elements (road, settlement and tea garden) that leads to high to very high landside hazard risk. The developed landslide hazard risk map of the Shivkhola Watershed exhibits a clear picture about the spatial location of vulnerability and risk of landslide hazard. The marginal parts and lower most segment of the basin experiences low intensity of risk elements and are also least affected by slope instability. Landslide hazard risk is very high at lower paglajhora, Shiviter Tea Garden Area, Tindharia etc. Lower Gyabari and Sepoydhura are the places of moderate to low probability of landslide hazard risk. Moderate level of risk is found at middle as well as lower section of the Shivkhola Watershed. It can be concluded that the watershed is dominated by the moderate to high level of landslide hazard risk. Landslide hazard risk is too high at Mahanadi, Tindharia and Shiviter because of higher intensity of the risk elements.

After thorough analysis of the intensity and magnitude of damage, 36 landslide events are marked as risky out of a total of 128 since 1968. Again the distribution of landslide among various landslide risk zone shows that very high, high and moderate risk areas experienced 62, 43 and 22 landslide events respectively and out of

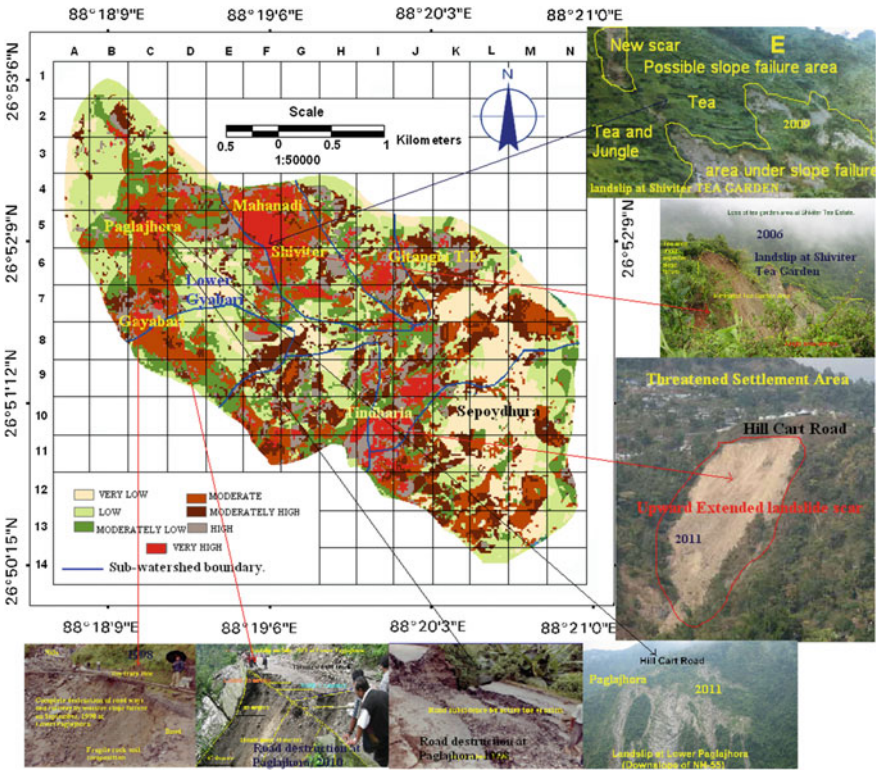

Fig. 7.11 Landslide hazard risk map with few significant risk events (field photo)

those 16, 13 and 7 are identified as riskful events. Frequency ratio for each low, moderate, high and very high landslide hazard risk zone are 0.00, 0.66, 1.42 and 2.48 respectively which also shows very low chance, tendency towards equal chance, high and very high chance of landslide hazard risk events in the respective hazard risk zones (Table 7.8). Analysis of frequency ratio conclude that there is a greater probability of future occurrence of risk events at the places of Lower Paglajhora, Tindharia and Shiviter in future and these three locations are presently existing in high to very high landslide hazard risk zone where frequency ratio is more than '1'.

The determined threshold slope angle of Paglajhora, Tindharia and Shiviter ranges from 13° to 37° and cohesion of the soil from 0.01 to 0.70 with greater percentage of sand particle. Very fragile and fragmented lithological composition helps easy percolation of rain water that generates adequate pore-water pressure for promoting downward movement of slope materials at Paglajhora and Tindharia. The existence of moderate to high intensity of risk elements and human intervention associated with all favourable geomorphic and geo-hydrologic landslide triggering

Table 7.8 Frequency ratio (FR) analysis and landslide probability for each risk zone

Landslide risk class	No. of pixels	Area (%)	Frequency landslide events	Frequency of risk event	Frequency of risk events (%)	Frequency ratio (FR)	Probability/chance of the risk event
Low (L)	8,982	27.34	1	0	0.00	0.00	Very low
Moderate (M)	9,641	29.35	22	7	19.44	0.66	Tendency towards equal
High (H)	8,333	25.37	43	13	36.11	1.42	High
Very high (VH)	5,888	17.92	62	16	44.44	2.48	Very high
Total	32,844	100	128	36	100		

factors have recognized Lower Paglajhora, Tindharia and Shiviter as high to very high landslide hazard risk zone in the Shivkhola Watershed.

The thickness of the soil and that of the saturated soil during monsoon are measured to be 4.5 m (Shiviter T.E.) and 7.25 m (Lower Paglajhora) and 1.28 m (Shiviter T.E) and 1.30 m (Lower Paglajhora) respectively at the back wall of the landslide scar though it is a bit lower further upslope on steeper section. The wet soil buck density is measured to be 1.96 g/cc and density of water is 1.07 g/cc. The angle of internal friction varies from 19° to 23° with an average of 21°. The calculated critical rainfalls of two major landslide prone parts of the Shivkhola watershed are 105.88 mm/day (Shiviter T.E.) and 88.93 mm/day (Lower Paglajhora) after Borga et al. (1998). Following Chow (1951, 1954, 1964) the calculated rainfall of 90.539 mm which is less than the critical rainfall of those two places at the recurrence interval of 1.01 year with 99 % probability.

The determined safety factor (FS) of all three locations are less than '1' which is measured considering the stress parameters such as major principal stress ($\boldsymbol{\sigma}_1$), minor principal stress ($\boldsymbol{\sigma}_3$), normal stress ($\boldsymbol{\sigma}_\mathbf{n}$), shear stress ($\tau$), angle of internal friction (Φ), cohesion (C), shear strength (λ), and rupture angle (α) applying Direct Shear Test Mechanism and developing Mohr's Stress Circle (Table 7.9). All the above mentioned parameters have recognized Paglajhora, Tindharia and Shiviter as significant unstable sections in the Shivkhola watershed. Not only that the slope steepening developed by road-cut benches and toe erosion, plying of heavy loaded vehicles and its enormous pressure on more fragile slope materials, depletion of forest cover in a rapid pace, continuous and regular orographic rainfall in rainy season, easy percolation of water through fragmented rock-soil composition and increase pore water pressure have caused destructive slope failure and damaged human structure and disrupted normal life by cutting-off the communication lines at all these three locations and have treated them as most significant landslide hazard risk prone sectors of the Shivkhola Watershed.

A comparative study has been made here to establish the interrelationship between all the landslide triggering factors (slope angle, slope curvature, slope aspect, lithology, drainage density, upslope contributing area, settlement density, road contributing area and land use and land cover.) considered in the present study as well as to figure out the different levels of abstraction of all the parameters in landslide hazard risk zones (Table 7.8). Study revealed that high and very high landslide hazard risk zones covering the places of Pahlajhora sinking zone, Tindharia, Shiviter, and 14 Miles Bustee are closely associated with 35–45° slope angle; north-east, south-east, north, east and south slope aspect; high posivite and high negative curvature; drainage density of 3.5–6.5 km/km^2; upslope area of more than 5 km^2; high settlement density; moderate to high road contributing area; and land use/land cover of settlement, road, degraded forest and open forest (Table 7.10).

Table 7.9 Measured geo-technical parameters for Tindharia, Shiviter and Paglajhora

Location	σ_3	σ_n	σ_1	τ	Φ	C	λ	α	F.S.
1. Tindharia Tea Garden	0.90	1.31818	2.15440	0.59036	19°28′	0.123	0.588929	35°16′	0.9975760
2. Lower Paglajhora (14 Miles Bustee)	0.82	1.28942	2.3212	0.69594	22°	0.149	0.6699594	34°	0.962668
3. Lower Paglajhora	0.96	1.4583	2.43794	0.6987	19°	0.162	0.6641329	35°30′	0.950526
4. Tindharia Rly. Stn.	0.92	1.4044	2.553	0.74598	24°	0.10 5	0.730279	33°	0.9789525
5. Shiviter T.E.	0.97	1.402407	2.3351579	0.63508	21°30′	0.07	0.6224228	34°15′	0.9800699

σ_1 = major principal stress; σ_3 = minor principal stress; σ_n = normal stress; τ = shear stress; Φ = angle of internal friction; C = cohesion; λ = shear strength; α = rupture angle; and F.S. = safety factor

Table 7.10 Comparative study between landslide triggering factors and landslide hazard risk zones

Hazard risk class	Lithology	Slope	Aspect	Curvature	Drainage density (km/km^2)	U.C.A (km^2)	Settlement density	R.C.A.	Land use/ land cover	Location
Very high	Gneiss/mica-schist	45°–70°	North/ east/ south	High Positive/ high negative	5–6.5	>10	>1.25	High	Degraded forest and settlement (20.11 and 12.55)	Lower pag-lajhora /shi-viter / Tindharia
High	Quatzite schist, phyllite	30°–45°	NE/SE	Moderate positive/ negative	3.5–5.5 and more than 8	5–10	0.5–1.25	Moderate to high	Road/mixed and open forest	/Gayabari/ 14 miles bu-stee/Nur-bong T.E Mahanadi/
Moderate	Soft sand-stone, shale	20°–30°	Flat	Low	2.00–3.50	<5	0.25–0.50	Low	Jungle	Giddapahar/ upper paglajhora
Low	Conglomerate/ shale/ sandstone	<20°	NW	Around (0)	<2.00	<5	<0.25	Low	Dense forest	Marginal/ mid-central part

UCA Upslope contributing area; *RCA* Road contributing area

Table 7.11 Accuracy assessment/comparison of landslide susceptibility with field data

Landslide hazard risk class	Classified total	Number correct	Producers correct	Users accuracy (%)	Accuracy total (%)
Very low	0.00	1	0	–	–
Low	0.00	1	0	–	–
Moderately low	0.00	3	0	–	–
Moderate	19	17	15	78.95	88.24
Moderately high	8	6	5	62.50	83.33
High	17	16	16	94.12	100.00
Very high	6	6	6	100.00	100.00
Total	50	50	42		
Overall classification accuracy = 92.89 %					
Overall Kappa statistics = 0.8929					

7.3.4 Accuracy Result of Landslide Hazard Risk Map

The comparison between assumed true data and randomly selected data from the classified image has been made on GIS Platform that shows the overall classification accuracy is 92.89 % and overall Kappa Statistics is 0.8929 %. The class wise accuracy result is shown in Table 7.11 that indicates acceptable results.

7.4 Conclusion

Very fragile and fragmented lithological composition helped easy percolation of rain water that generated adequate pore-water pressure for promoting downward movement of slope materials at Paglajhora and Tindharia. The combinations of moderate to high intensity of risk elements and human intervention associated with all favourable geomorphic and geo-hydrologic landslide triggering factors have recognized Lower Paglajhora, Tindharia and Shiviter as high to very high landslide hazard risk zone in the Shivkhola Watershed. The calculated critical rainfalls of two major landslide prone parts of the Shivkhola watershed are 105.88 mm/day (Shiviter T.E.) and 88.93 mm/day (Lower Paglajhora) after Borga et al. (1998). Log probability analysis after Chow (1951, 1954, 1964) shows that the rainfall of 90.539 mm is expected at the recurrence interval of 1.01 year with 99 % probability. This revealed high-potentiality of slide at these locations. Not only that, the slope steepening caused by road-cut benches and toe erosion, plying of heavy loaded vehicles, depletion of forest cover in a rapid pace, continuous and regular orographic rainfall in rainy season, easy percolation of water through fragmented rock-soil composition and increase pore water pressure have caused destructive slope failure at all these three locations.

The derived prioritized factor rating values (PFRV) were high for Slope steepness (0.2944), lithology (0.2150), drainage (0.1537), and lineaments (0.1087) indicating as the significant contributing factors for landsliding in the Shivkhola watershed. The slope aspect, settlement density and LULC were registered with minimum prioritized factor rating values of 0.0149, 0.0193 and 0.0266 that proved these factors as less significant to promote landslide activities. Road contributing area (RCA), slope curvature and upslope contributing area were proved to be moderately important in the present context. Analytical hierarchy process is proved to be important to efficiently identify the landslide triggering factors of most importance. It may again be helpful as a support in decision making process for efficient management. The study revealed that lithological composition with steep slope and drainage network orientation are to be given more priority in the decision of structural construction, specially the construction of roads.

References

Anabalagan R (1992) Landslide hazard evaluation and zonation mapping in mountainous terrain. Eng Geol 32:269–277

Atkinson PM, Massari R (1998) Generalized linear modeling of susceptibility to landsliding in the central Apennines, Italy. Comput Geosci 24:373–385

Avinash KG, Ashamanjari KG (2010) A GIS and frequency ratio based landslide susceptibility mapping: Aghnashini river catchment, Uttara Kannada, India. Int J Geomat Geosci 1 (3):343–354

Basu SR, Sarkar S (1985) Some consideration on recent landslides at Tindharia and their control, Indian. J Power River Valley Dev 1985:190–194

Basu SR, Sarkar S (ed) (1988) Ecosystem visavis Landslides, a case study in Darjeeling Himalayas. Impact of development on environment. Geog Soc India Cal II:45–53

Basu SR, Ghatowar L (1988) Landslides and soil erosion in the gish drainage basin of the Darjeeling Himalaya and their bearing on North Bengal floods. Studia Geomorph Carpatho Bale 22:105–22

Basu SR, Ghosh L (1993) A comprehensive study of landslides and floods in the lish basin of the Darjeeling Himalaya, Indian J Power River Valley Dev 43:196–203

Basu SR, Maiti RK (2001) Unscientific mining and degradation of slopes in the Darjeeling Himalayas. Chang Env Scenerio Indian Subcont (Bd) 390–399

Borga M et al (1998) Shallow landslide hazard assessment using a physically based model and digital elevation data. J Environ Geol 35(2–30):81–88

Brardinoni F, Church M (2004) Representing the landslide Magnitude Frequency relation; Capilano river basin, British Colombia. Kirkby JM, Darby ES (eds) Earth surface processes and landforms, vol 29, issue 1, pp 115–124

Brudsen D (1979) Mass movement. In: Embelton C, Thornes J (eds) Process in geomorphology. Wiley, New York, pp 130–186

Burton A, Bathurst JC (1998) Physically based modeling of shallow landslide erosion and sediment yield at a catchment scale. Environ Geol 35(2–3):89–99

Caiyan WU, Jianping Q (2009) Relationship between landslides and lithology in the three Gorges reservoir area based on GIS and information value model, vol 42, issue 2. Higher Education Press and Springer, pp 165–170

Carson MA (1975) Threshold and characteristic angles of straight slopes. In: Proceedings of the 4th Guelph symposium on geomorphology, Norweich Geo Books, pp 19–34

Carson MA (1977) Angles of repose, angles of shearing resistance at angle of talus slopes. Earth Surf Processes 2:363–380
Catlos EJ, Harrison TM, Kohn MJ, Grove M, Ryerson FJ, Manning CE, Upreti BN (2001) Geochronologic and thermobarometric constraints on the evolution on the main central thrust, central Nepal Himalaya. J Geophys Res 106:16177–16204
Chow VT (1951) General formula for hydrologic frequency analysis. Am Geophys Union Trans 32:231–237
Chow VT (1954) The long-probability law and its engineering applications. ASCE 80:1–25 (Separate No. 536)
Chow VT (ed) (1964) Handbook of applied hydrology. Mc Grow-Hill Book Company, New York
Congalton R (1991) A review of assessing the accuracy of classification of remotely sensed data. Remote Sens Environ 37:35–46
Crozier MJ (1986) Landslides: causes, consequences and environment. Croom Helm Australia Pty Ltd., London, 252p
Dai FC, Lee CF (2002) Landslide characteristics and slope instability modeling using GIS; Lantau Island, Hong Kong. Geomorphology 42:213–228
Dhakal AS, Amada T, Aniya M (2000) Landslide hazard mapping and its evaluation using GIS: an investigations of sampling schemes for a grid-cell based quantitative method. Photogram Eng Remote Sens 66(8):981–989
Donati L, Turrini MC (2002) An objective and method to rank the importance of the factors predisposing to landslides with the GIS methodology, application to an area of the Apennines (Valnerina; Perugia, Italy). Eng Geol 63:277–289
Dutta KK (1966) Landslips in Darjeeling and neighbouring hills slopes in June 1950. Bulletin of the geological survey of India. Ser B 15(1):7–30
Einstein HH (1988) Landslide risk assessment procedure. In: Proceedings of the fifth international symposium on landslides, pp 1075–1090
Ghosh S, Van Westen CJ, Carranza E, Jetten V (2009) Generation of event- based landslide inventory maps in a data-scarce environment; case study around Kurseong, Darjiling district, West Bengal, India. In: Malet JP, Remaitre A, Bogaard T (eds) Landslide processes: from geomorphologic mapping to dynamic modeling: proceedings of the landslide processes. European centre on geomorphological hazards (CERG), Strasbourg, pp 37–44
Gokceoglu C, Sonmez H, Ercanoglu M (2000) Discontinuity controlled probabilistic slope failure risk map of the Altindag (settlement) region in Turkey. Eng Geol 55:277–296
Guzzetti F, Carrara A, Cardinali M, Reichenbach P (1999a) Landslide hazard evaluation: a review of current techniques and their application in a multi-scale study, Central Italy. J Geomorphol 31:181–216 (Elsevier, London)
Guzzetti F, Cardinali M, Reichenbach P, Carrara A (1999b) Comparing landslide maps; a case study in the upper Tiber River basin, central Italy. Environ Manage 18:623–633
Guzzetti F, Cardinali M, Reichenbach P, Carrara A (1999c) Landslide hazard evaluation: an aid to a sustainable development. Geomorphology 31:181–216
Intarawichian N, Dasananda S (2011) Frequency Ratio model based landslide susceptibility mapping in lower Mae Chaem watershed, Northern Thailand. Environ Earth Sci 64:2271–2285
Jadda M (2009) Landslide susceptibility evaluation and factor analysis. Eur J Sci Res 1450-216X33(4):654–668
Jibson WR, Edwin LH, John AM (2000) A method for producing digital probabilistic seismic landslide hazard maps. Eng Geol 58:271–289
Kamp U, Growley BJ, Khattak GA, Owen LA (2008) GIS based landslide susceptibility mapping for the 2005 Kashmir earthquake region. Geomorphology 101:631–642
Komac M (2006) A landslide susceptibility model using the analytical hierarchy process method and multivariate statistics in perialpine Slovenia. Geomorphology 74:17–28
Lee S, Choi U (2003) Development of GIS based geological hazard information system and its application for landslide analysis in Korea. Geosci J 7:243–252

Lee S, Ryu JH, Won JS, Park HJ (2004a) Determination and publication of the weights for landslide susceptibility mapping using an artificial neural network. Eng Geol 71:289–302

Lee S, Choi J, Min K (2004b) Probabilistic landslide hazard mapping using GIS and remote sensing data at Boun, Korea. Int J Remote Sens 25:2037–2052

Lee S, Pradhan B (2006) Landslide hazard assessment at Cameron highland Malaysia using frequency ratio and logistic regression models. Geophys Res Abs 8. SRef-ID: 1607-7962/gra/EGU06-A-03241

Lee S, Pradhan B (2007) Landslide hazard mapping at Selangor, Malaysia using frequency ratio and logistic regression models. Landslides 4(1):33–41

Lee S, Talib JA (2005) Probabilistic landslide susceptibility and factor effect analysis. Environ Geol 47:982–990

Maiti RK (2007a) Irrational resource extraction introducing instability in slope and hydrodynamics- a case study at Lish-Chunkhola basin, Darjiling, Indian. J Geogr Environ 8&9:41–51 Vidyasagar University

Maiti RK (2007b) Critical analysis of slope instability on mining scars at Tindharia Cricket Colony, Darjiling, West Bengal. In: Proceedings of eighteenth convention and national seminar on "quarternary" climatic changes and landforms, organized at Manonmaniam Sundaranar University, Tirunelveli, Tamilnadu, pp 189–205

Mallet FR (1875) On the geology and mineral resources of the Darjeeling district and Western Duars. Mem Geol Surv India 2:1–72

Mandal S, Maiti R (2011) Landslide susceptibility analysis of Shivkhola watershed, Darjiling: a remote sensing and GIS based analytical hierarchy process (AHP). J Indian Soc Remote Sens. doi:10.10007/s12524-011-0160-9

Mandal S, Maiti R (2012) Application of RS and GIS based semi-quantitative approach in landslide hazard risk assessment of the Shivkhola watershed, Darjiling Himalaya. Geo Risk Assess Manag Risk Eng Syst Geohazards 6(4):203–220

Mandal S, Maiti R (2013) Integrating the analytical hierarchy process (AHP) and the frequency ratio (FR) model in landslide susceptibility mapping of Shiv-khola watershed, Darjeeling Himalaya. Int J Disaster Risk Sci 4(4):200–212

Muthu K, Petrou M (2007) Landslide hazard mapping using an expert system and a GIS. IEEE Trans Geosci Remote Sens 45(2):522–531

Mwasi B (2001) Land use conflicts resolution in a fragile ecosystem using multi criteria evaluation (MCE) and a GIS based Decision Support System (DSS)

Nie et al (2001) The application of remote sensing technique and AHP-fuzzy method in comprehensive analysis and assessment for regional stability of Chongqing City, China. In: Proceedings of the 22nd international Asian conference on remote sensing, vol 1. University of Singapore, Singapore, pp 660–665, 5–9 Nov 2001

Nithya ES, Prasanna RP (2010) An integrated approach with GIS and remote sensing technique for landslide zonation. Int J Geomatics Geosci 1(1):66–75

Pandey A, Dabral PP, Chowdhary VM, Yadav NK (2008) Landslide hazard zonation using remote sensing and GIS: a case study of Dikrong river basin, Arunachal Pradesh, India. Environ Geol 54:1517–1529

Pistocchi A, Luzi L, Napolitano P (2002) The use of predictive modeling techniques for optimal exploitation of spatial databases: a case study in landslide hazard mapping with expert system-like methods. Environ Geol 41:765–775

Porghasem H (2007) Landslide hazard zoning statistical frequency ratio method in the basin Safarood. M.Sc thesis, Tarbiat Modarres University, Noor, pp 1386

Pradhan B, Lee S (2010a) Delineation of landslide hazard areas on Penang Island, Malaysia, by using frequency ratio, logistic regression, and artificial neural network models. Environ Earth Sci 60:1037–1054

Pradhan B, Lee S (2010b) Landslide susceptibility assessment and factor effect analysis: backpropagation artificial neural networks and their comparison with frequency ratio and bivariate logistic regression modeling. Environ Models Softw 25(6):747–759
Pradhan B, Lee S (2010c) Regional landslide susceptibility analysis using back-propagation neural network model at Cameron highland, Malaysis. Landslides 7(1):13–30
Parise M, Jibson WR (2000) A seismic landslide susceptibility rating of geologic units based on analysis of characteristics of landslides triggered by the 17 January, 1994 Northridge, California earthquake. Eng Geol 58:251–270
Quinn et al (1991) The prediction of hillslope flow paths for distributed hydrological modeling using digital terrain models. Hydro Processes 5:59–79
Rowbotham D, Dudycha DN (1998) GIS modelling of slope stability in Phewa Tal watershed, Nepal. Geomorphology 26:151–170
Saaty TL (1980) The analytical hierarchy process. McGraw Hill, New York, 350p
Saaty TL (1990) The analytical hierarchy process: planning, priority setting, resource allocation, 1st edn. RWS Publication, Pittsburgh, 502p
Saaty TL (1994) Fundamentals of decision making and priority theory with analytic hierarchy process, 1st edn. RWS Publication, Pittsburgh, 527p
Saaty TL, Vargas LG (2001) Models, methods, concepts and applications of the analytic hierarchy process, 1st edn. Kluwer Academic, Boston, 333p
Sarkar S, Kanungo DP (2004) An integrated approach for landslide susceptibility mapping using remote sensing and GIS. Photogram Eng Remote Sens 70(5):617–625
Sharifikia M (2007) RS and GIS application in Geo-hazard- A case study part of central Alborz-Iran. Ph.D. thesis submitted in Geology Department, University of Delhi, India
Sinha-Roy S (1982) Himalayan main central thrust and its implication for Himalayan inverted metamorphism. Tectonophysics 84:197–224
Soeters R, Westen CJ (1996) Slope instability recognition, analysis and zonation. In: Turner AK and Schuster RL (eds) Landslides: investigation and mitigation. transportation research board special report 247. National Academy Press, Washington, DC, pp 129–177
Tiwari B, Marui H (2001) Shearing behaviour of landslide sliding and mining scarp soil during drained ring shear test. In: Proceedings of XVth international conference on soil mechanics and geotechnical engineering, vol 1, Istambul, pp 295–298
Tiwari B, Marui H (2002) Mechanism of shear zone formation and its effect in residual shear strength. In: Proceedings of 3rd international conference on landslides, slope stability and safety of infrastructure, vol 1, pp 4–133
Tiwari B, Marui H (2003) Estimation of residualshear strength for bentonite-kaolin-Toyoura sand mixture. J Japn Landslide Soc 40(2):124–133
Tiwari B, Marui H (2004) Objective oriented multi-stage ring shear test for the shear strength of the landslide soil. J Geotech Geoenviron Eng ASCE 130(2):217–222
Van Westen CJ, Castellanos Abella E, Sekhar LK (2008) Spatial data for landslide susceptibility, hazards and vulnerability assessment: an overview. Eng Geol 102(3–4):112–131
Varnes DJ (1958) Landslide types and processes. In: Eckel EB (ed) Landslides engineering practice: highway research board, special report 29, vol 544. NAS-NRC Publication, Washington, DC, pp 20–47
Vanmarcke EH (1977) Reliability of earth slopes. J Geotechl Eng Div ASCE 103 (GT11):1247–126
Varnes DJ (1984) Landslide hazard zonation review of principle and practice. Natural hazards, UNESCO, Paris
Vijith H, Madhu G (2008) Estimating potential landslide sites of an upland sub-watershed in Western Ghat's of Kerala (India) through frequency ratio and GIS. Environ Geol 55:1397–1405
Windisch EJ (1991) The hydraulics problem in slope stability analysis. Can Geotech J 28 (6):903–909

Yagi H (2003) Development of assessment method for landslide hazardness by analytical hierarchy process (AHP). Abstract volume of the 42nd annual meeting of the Japan Landslide Society, pp 209–212

Yalcin A, Bulut F (2007) Landslide susceptibility mapping using GIS and digital photogrammetric techniques: a case study from Ardesen (NE Turkey). Nat Hazard 41(1):201–226

Yalcin A (2008) GIS based landslide susceptibility mapping using analytical hierarchy process and bivariate statistics in Ardesen (Turkey): comparisons of results and confirmations. Catena 72:1–12

Young A (1963) Deductive models of slope evolution. Rep Int Geogr Un Slopes Comm 3:45–66

Zhou CH, Lee CF, Li J, Xu ZW (2002) On the spatial relationship between landslide and causative factors on Lantau Island, Hong Kong. Geomorphology 43:197–207